

Magplane Guideway and LSM Heat Transfer

Jiarong Fang and Min Chen

MIT Plasma Science and Fusion Center, Cambridge, MA, U.S.A.

D. Bruce Montgomery

Magplane Technology, Inc., Bedford, MA, U.S.A.

ABSTRACT: A one-dimension heat transfer model was developed to calculate the temperature rise and distribution along the guideway conductive sheets caused by drag forces of the lift pads and the LSM windings caused by the resistive loss of the propulsion currents. We assume that an urban Magplane line has a station for every 3km of guideway distance, and a 5-section Magplane car set leaves a station at intervals of 90s with a levitation gap of 5cm in the acceleration section. Models for forced-flow air cooling or natural convection induced flow in inclined parallel channels are examined with the goal of controlling the temperature rise of the initial two 150 meter sections of the LSM windings at the exit ramp of each station.

1 INTRODUCTION

The Magplane vehicle magnetics are modeled as a symmetric 10 wavelength propulsion array located at the center of the vehicle bottom, and four identical 2 wavelength lift pads symmetrically located at four corners of the vehicle. The lift pads have the same tilt angle of 37° relative to the vertical plane of the arc-shaped guideway [1-2].

The temperature fluctuations in the guideway and LSM windings of Magplane [3] can be caused by the surrounding temperature swings, the sun rays, emergency braking, electromagnetic drag forces, and LSM resistive loss. Here we only consider the effect of drag forces of the lift pads and LSM resistive loss, assuming that the surrounding temperature keeps at 30°C .

2 HEAT TRANSFER EQUATIONS

There are three kinds of heat transfer involved including heat conduction, heat convection, and radiation heat transfer. The heat flow equation operating on the guideway or LSM windings may be given by

$$\rho V C_p \frac{\partial T}{\partial t} = \nabla \cdot (k_c \nabla T) \cdot V + q_j + q_d - q_c - q_r \quad (1)$$

The left side of the above Equation 1 represents the time rate of change of thermal energy of the

guideway or LSM windings, ρ is the mass density of the guideway or LSM windings, V is the volume, and C_p is the heat capacity of the guideway or LSM windings. The first term in the right-hand side of Equation 1 represents the conduction heat flow into the guideway element or LSM winding element, where k_c is the guideway element's thermal conductivity or the LSM winding element's thermal conductivity, q_j represents the Joule heating generated in the guideway caused by the drag forces of lift pads or the LSM windings caused by the resistive loss of LSM currents when the train passes over the guideway, q_d represents the heat generation other than by q_j , q_c is the convection heat transfer, and q_r is the radiation heat transfer.

Here for computational simplicity, we assume that the vehicle runs at a constant speed of v , and all the heat generation caused by the drag forces of lift pads and the resistive loss of LSM windings will be dissipated uniformly in the guideway and LSM windings, so there is no heat conduction, and both heated upper and lower surfaces have the same temperature. Considering the headway time of t_H , the Joule heating generated in the guideway caused by the drag forces of lift pads can be expressed by

$$q_j = F_d \cdot v / t_H \quad (2)$$

where F_d is the sum of drag forces of lift pads, and the Joule heating generated in the LSM wind-

ings caused by the resistive loss of LSM windings can be represented by

$$q_j = 3I^2 R / t_H \quad (3)$$

where I is the phase current in the LSM, and R is the resistance of one phase of the LSM windings.

During the headway interval time, there are no vehicles passing over a given section of the LSM windings, so the heat convection conditions could be considered to be natural still air. The rate of heat transfer by natural convection from the solid surface at a uniform temperature T_s to the surrounding fluid is expressed by Newton's law of cooling as

$$q_c = h_c \cdot A_s (T_s - T_\infty) \quad (4)$$

where h_c is the convection heat transfer coefficient, A_s is the surface area, and T_∞ is the temperature of the quiescent fluid away from the surface.

Radiation will be significant for most systems cooled by natural convection. Therefore, a radiation analysis should normally accompany a natural convection analysis unless the emissivity of the surfaces is low [4]. The rate of radiation heat transfer can be given by

$$q_r = \varepsilon \cdot \sigma \cdot A_s [(T_s + 273)^4 - (T_\infty + 273)^4] \quad (5)$$

where ε is the emissivity, and σ is the Stefan-Boltzmann constant with the value of $5.669 \times 10^{-8} \text{ W/m}^2 \cdot \text{K}^4$.

3 GUIDEWAY HEAT TRANSFER CAUSED BY DRAG FORCES OF LIFT PADS

3.1 Combined Free Convection and Radiation Heat Transfer Coefficient

Here for computational simplicity, the arc-shaped Magplane guideway can be simplified as the two inclined surfaces. As shown in Figure 1, we assume

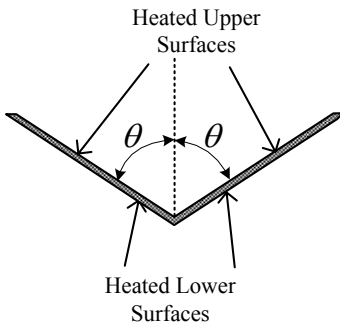


Figure 1. Cross-section view of simplified guideway

that the heat generation caused by the drag forces of lift pads will be dissipated uniformly in the guideway conductive sheets, and that the guideway concrete trough can be neglected, and both upper and

lower surfaces of guideway have been treated as heated surfaces with the same temperature. For an inclined plate with the heated surface facing downward with approximately constant heat flux, the empirical correlations for the average Nusselt number can be expressed as

$$Nu_{e1} = 0.56 (Gr_e Pr_e \cos \theta)^{1/4} \quad (6)$$

For the angle $\theta < 88^\circ$, $10^5 < Gr_e Pr_e \cos \theta < 10^{11}$ [5], where Pr_e is the Prandtl number, and the Grashof number Gr_e can be given by

$$Gr_e = \frac{g \beta (T_s - T_\infty) L_c^3}{\nu^2} \quad (7)$$

where g is the gravitational acceleration, L_c is the characteristic length of inclined plate, ν is the kinematic viscosity of the fluid, and the reference temperature T_e can be defined by

$$T_e = T_s - 0.25(T_s - T_\infty) \quad (8)$$

and coefficient of volume expansion β is

$$\beta = \frac{1}{T_\infty + 0.25(T_s - T_\infty) + 273} \quad (9)$$

For an inclined plate with the heated surface facing upward, the empirical correlations for the average Nusselt number can be modified from Equation 6 to

$$Nu_{e2} = 0.14 [(Gr_e Pr_e)^{1/3} - (Gr_e Pr_e)^{1/3}] + 0.56 (Gr_e Pr_e \cos \theta)^{1/4} \quad (10)$$

For the angle $15^\circ < \theta < 75^\circ$, $10^5 < Gr_e Pr_e \cos \theta < 10^{11}$, where Gr_e is the critical Grashof relation indicating when the Nusselt number starts to separate from the laminar relation of Equation 6.

Considering the radiation heat transfer, the combined heated upper and lower surface convection and radiation heat transfer coefficient can be determined from

$$h = \frac{k}{L_c} (Nu_{e1} + Nu_{e2}) + \frac{\varepsilon \sigma [(T_s + 273)^4 - (T_\infty + 273)^4]}{T_s - T_\infty} \quad (11)$$

where k is the thermal conductivity of the fluid.

We assume that the surrounding temperature keeps at 30°C , the emissivity of the aluminum guideway $\varepsilon = 0.4$, and the angle $\theta = 53^\circ$ which the sloped guideway makes with the vertical, and use above Equations 6-11 to calculate the combined free convection and radiation heat transfer coefficient. Figure 2 shows both lower surface and upper surface

heat transfer coefficient, radiation heat transfer coefficient, and combined free convection and radiation heat transfer coefficients vs. temperature difference ΔT . It seems that the upper surface of the sloped guideway has more efficient heat transfer than the lower surface, and the radiation heat transfer is comparable to the lower surface even with the small guideway emissivity of $\varepsilon=0.4$.

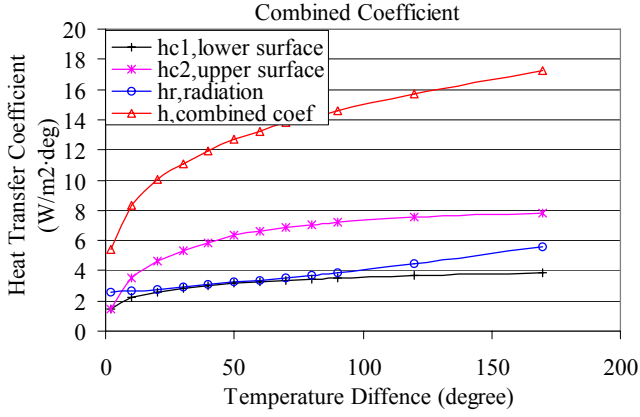


Figure 2: Combined Coefficients vs. Temperature Difference ΔT

3.2 Steady State Analyses

For steady state analyses, assume there is no heat conduction and no heat generation other than the Joule heating generated in the aluminum guideway caused by the drag forces of lift pads, Equation 1 may become

$$0 = 0 + q_j + 0 - q_c - q_r \quad (12)$$

Using Equation 2 and the combined heat transfer coefficient as described in Equation 11, we can calculate the equilibrium temperature T_{equ} from the following equation:

$$T_{equ} - T_{\infty} = \frac{F_d}{2hL_c t_H} \quad (13)$$

where h is the combined free convection and radiation heat transfer coefficient, and can be calculated by the curve of combined coefficient vs. temperature difference.

Table 1: Guideway steady-state temperature rise with 5-section Magplane train at different constant speeds (surrounding temperature $T_{\infty}=30=C$)

Speed (m/s)	Drag Force (5 sections) (N)	5-Section, Headway $t_H=90s$	
		q_j/A_s convective (W/m ²)	$T_{equ} - T_{\infty}$ (=C)
20	191,200	708.0	54.6
30	162,400	601.5	47.9
50	144,000	533.5	43.6
100	126,400	468.0	39.3
150	113,475	420.5	36.1

As seen from Equation 13, the guideway temperature rise is proportional to the drag force and vehicle passing frequency. Table 1 shows the guideway steady-state temperature rise for a 90 second headway with 5-section Magplane train at different constant speeds. The lower the speed is, the higher the drag forces and the temperature rise are. For a 5-section train with 90 second headway the maximum temperature is a manageable 85=C.

4 LSM HEAT TRANSFER CAUSED BY RESISTIVE LOSS AT LOW SPEEDS

4.1 Combined Free Convection and Radiation Heat Transfer Coefficient

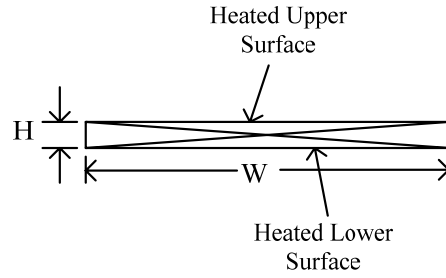


Figure 3. Cross-section view of simplified LSM windings

As shown in Figure 3, the LSM windings can be simplified as the horizontal plate. Similar to the guideway conductive sheet calculation, we assume that the heat generation caused by the resistive loss of LSM windings will be dissipated uniformly in the LSM windings, and both upper and lower surfaces of LSM windings can be treated as heated surfaces with the same temperature. For a horizontal plate with the heated surface facing downward, the empirical correlations for the average Nusselt number can be expressed as

$$Nu_{L1} = 0.27 Ra_L^{1/4} \quad (14)$$

For $10^5 \leq Ra_L \leq 10^{10}$ [6], where Ra_L is the Rayleigh number, which can be given by

$$Ra_L = \frac{g\beta(T_s - T_{\infty})L^3}{\nu\alpha} \quad (15)$$

where α is the thermal diffusivity, the characteristic length of horizontal plate, L , can be defined by

$$L = \frac{A_s}{P} \approx W/2 \quad (16)$$

where W is the width of LSM windings, A_s and P are the plate surface area and perimeter, respectively, and coefficient of volume expansion β is

$$\beta = \frac{1}{0.5(T_s + T_\infty) + 273} \quad (17)$$

For a horizontal plate with the heated surface facing upward, the empirical correlations for the average Nusselt number can be determined by

$$\begin{cases} Nu_{L2} = 0.54 Ra_L^{1/4} & (10^4 \leq Ra_L \leq 10^7) \\ Nu_{L2} = 0.15 Ra_L^{1/3} & (10^7 \leq Ra_L \leq 10^{11}) \end{cases} \quad (18)$$

Considering the radiation heat transfer, the combined heated upper and lower surface free-convection and radiation heat transfer coefficient can be determined from

$$h = \frac{k}{L}(Nu_{L1} + Nu_{L2}) + \frac{\varepsilon\sigma[(T_s + 273)^4 - (T_\infty + 273)^4]}{T_s - T_\infty} \quad (19)$$

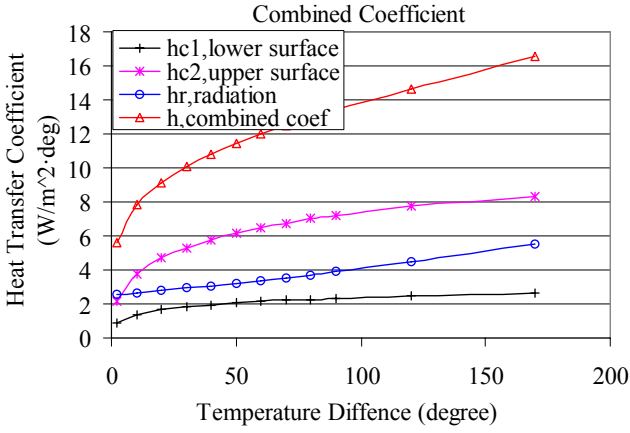


Figure 4: Combined Coefficients vs. Temperature Difference ΔT

Figure 4 shows both lower surface and upper surface heat transfer coefficient, radiation heat transfer coefficient, and combined free convection and radiation heat transfer coefficients vs. temperature difference ΔT . It seems that the upper surface of the LSM windings has almost two times more efficient heat transfer than the lower surface, and the radiation heat transfer is comparable to the lower surface. In comparison with the corresponding calculation results of heat transfer coefficients of inclined guideway model as shown in Figure 2, the radiation heat transfer coefficients are same, free convection heat transfer coefficients of upper surface are very close, but lower surface heat transfer coefficients of LSM windings are about 30% smaller, so the combined free convection and radiation heat transfer coefficients are about 10% less than the corresponding heat transfer coefficients of inclined guideway.

4.2 Steady State Analyses

For steady state analyses, using Equation 3 and the combined heat transfer coefficient as described in

Equation 19, we can simply calculate the equilibrium temperature T_{equ} from the following equation:

$$T_{equ} - T_\infty = \frac{3I^2 R}{hW \nu t_H} \quad (20)$$

where ν is the vehicle running speed, and h is the combined free convection and radiation heat transfer coefficient, which can be calculated by the curve of combined coefficient vs. temperature difference.

4.3 Transient Process

From Equation 1, and in this transient calculation assuming one layer of concrete guideway underneath the LSM windings, the one-dimension heat transfer equation may be simplified as

$$\rho_c A_c C_c \frac{\partial T}{\partial t} = \frac{\partial}{\partial x} [k_c A_c \frac{\partial T}{\partial x}] + q_j + q_d - q_c - q_r \quad (21)$$

where

$$\rho_c A_c C_c = \rho_{LSM} C_{LSM} \delta_{LSM} W_{LSM} + \rho_{con} C_{con} \delta_{con} W_{con} \quad (22)$$

$$\text{and } k_c A_c = k_{LSM} \delta_{LSM} W_{LSM} + k_{con} \delta_{con} W_{con} \quad (23)$$

where δ is thickness, W is width, and the subscripts c , LSM , and con refer to composite, LSM windings, and concrete, respectively.

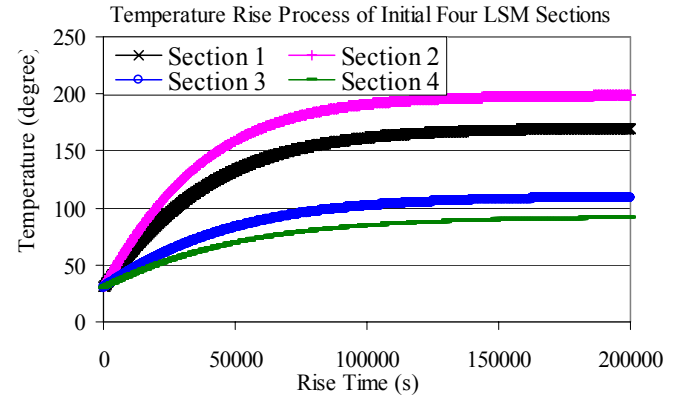


Figure 5: Temperature Rise Process of Initial Four Sections of LSM Windings

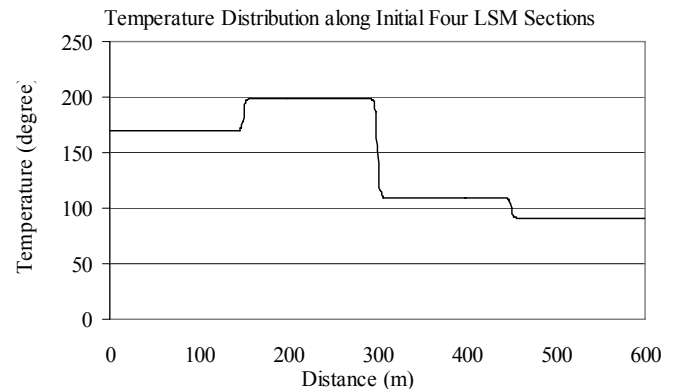


Figure 6: Steady-State Temperature Distribution along the LSM Windings

Using above three equations, we can simulate the transient process of one-dimension heat transfer of composite LSM windings and concrete guideway. Here we take an urban Magplane line as an example, and assume that a Magplane line has a station for every 3km of guideway distance, and a 5-section Magplane train leaves a station at intervals of 90s with a levitation gap of 5cm between the face of the propulsion magnet and face of the LSM winding. The 5-section Magplane train is accelerated to the desirable top cruising speeds at the constant acceleration rate of 0.1g, keeps constant at the cruising speed, then is decelerated to the stop at the deceleration rate of -0.1g, and the total traveling distance is 3km between two neighboring stations.

The typical section length of LSM stators is 150m, and two neighboring sections of LSM stators are electrified simultaneously. Figure 5 shows the temperature rise process of the initial four sections of LSM windings. The temperature is increasing in an exponential way, and it takes almost 42 hours (~150,000 seconds) to reach the steady-state temperature. The final steady-state temperature distribution along the initial four sections of the LSM windings is shown in Figure 6, and it seems that each section of LSM windings will be uniformly heated up to the almost same temperature except the two ends which are contiguous to the other section with different temperatures.

As seen from Figure 5, the temperature of the LSM's Section 2 may go beyond the allowable temperature limitation for the LSM rubber-insulated cables after continuous heating of only 4 hours (~15,000 seconds); however, only the initial two sections will require some form of cooling to mitigate the heating. We consider two potential methods to reduce the temperature of the initial two sections, forced-flow air cooling and natural convection using inclined parallel channels.

5 LSM'S FORCED-CONVECTION HEAT TRANSFER BY AIR FLOW

5.1 Forced-Flow Cooling

As shown in Figure 7, the LSM windings and

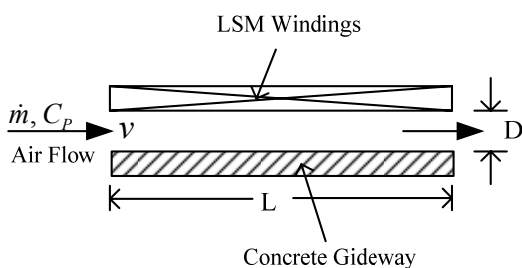


Figure 7. Side view of Forced-Flow Cooling Channel

concrete guideway span can be simplified as horizontal plates, where L is the length of the span, taken as 30 meters in our calculations. We assume that the heat generation caused by the resistive loss of LSM windings will be dissipated uniformly in the LSM windings and concrete guideway, and the air flow is forced to go through the rectangle channel between LSM windings and the concrete guideway at the speed of v , in order to cool down the LSM windings and concrete guideway.

The upper surface of LSM windings is exposed to the air, so it can be treated as natural convection with heated upper surface. For a horizontal plate with the heated surface facing upward, the empirical correlations for the average Nusselt number can be determined by

$$\begin{cases} Nu_L = 0.54Ra_L^{1/4} & (10^4 \leq Ra_L \leq 10^7) \\ Nu_L = 0.15Ra_L^{1/3} & (10^7 \leq Ra_L \leq 10^{11}) \end{cases} \quad (24)$$

Considering the radiation heat transfer, the combined free convection of upper heated surface of LSM windings and radiation heat transfer coefficient can be determined by

$$h_c = \frac{k}{L_c} Nu_L + \frac{\varepsilon\sigma[(T_s + 273)^4 - (T_\infty + 273)^4]}{T_s - T_\infty} \quad (25)$$

For the forced-flow cooling, the rate of forced-convection heat transfer can be given by

$$q_f = h_f A_s (T_w - T_f) = \frac{k_f Nu_f}{D} A_s (T_w - T_f) \quad (26)$$

The subscript f refers to flow coolant (air) and D is an equivalent hydraulic diameter of the channel, which can be defined by

$$D = \frac{4A_f}{P_f} \quad (27)$$

where A_f is the cross-sectional area of the channel and P_f are the channel perimeter.

For the fully developed turbulent flow ($Re_f \geq 3000$) and laminar flow ($Re_f < 3000$), where Re_f is the air Reynolds number, the air Nusselt number can be determined respectively by

$$Nu_f = 0.023 Re_f^{0.8} Pr^{0.3} \quad Re \geq 3000 \quad (28)$$

$$Nu_f = 3.66 + \frac{0.0668(D/L)Re_f Pr}{1 + 0.04[(D/L)Re_f Pr]^{2/3}} \quad Re < 3000 \quad (29)$$

where Pr is the air Prandtl number, and L is the channel length.

5.2 Transient Process

We suppose that the forced-flow channel takes the same length as the guideway span of 30m. Figure 8 compares the temperature rise process of the initial two sections of LSM windings cooled by air flow at different speeds (channel length=30m). It can be seen from the figure that after 65,000 seconds (18 hours), which is the usual operation time of urban transportation systems from 6:00AM to 12:00PM, the average temperature of each of initial two forced-cooling LSM windings will be dropped by ~20 degrees (e.g. for section 1, from 115 degree to 94 degree) when increasing the cooling flow speed from 5m/s to 10m/s; if we continue to increase the cooling flow speed from 10m/s to 20m/s, the average temperature will be decreased by an additional 20 degrees. Figure 9 shows the corresponding LSM and flow temperature distribution along the initial four sections of LSM windings with initial two sections cooled with different air flow speeds. It can be seen from the figure that the increase of flow speed will help to decrease the temperature of both LSM windings and the air flow within channels. As shown in Figure 9, however, even using 20m/s forced flow cooling, there are some parts of the LSM windings that are still beyond the allowable temperature limitation for LSM insulated rubber cables. We therefore do not consider forced flow air cooling along the length of the spans to be a practical solution.

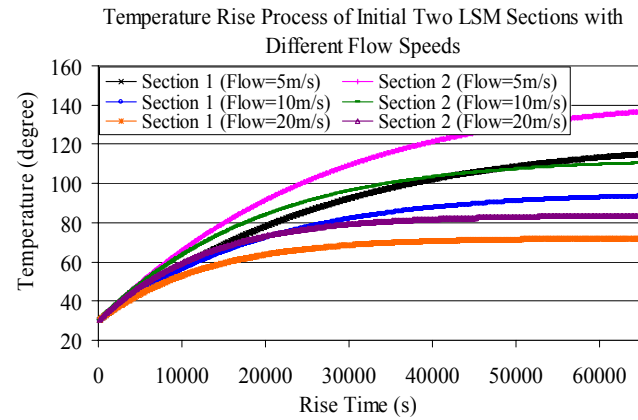


Figure 8: Comparison of Temperature Rise Process of Initial Two Sections of LSM Windings Cooled by Air Flow at Different Speeds (Channel Length=30m)

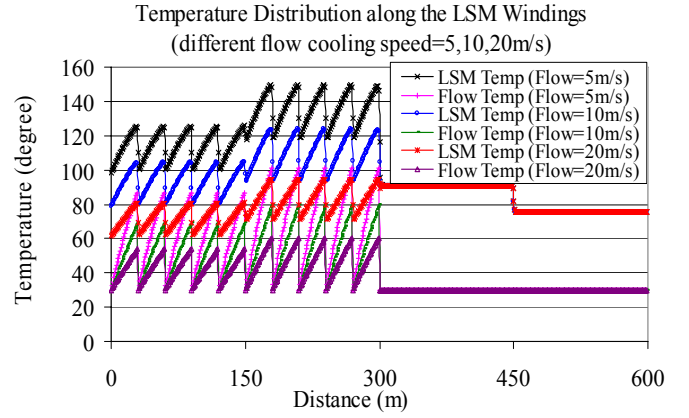


Figure 9: Comparison of LSM and Flow Temperature Distribution along the Initial Four LSM Windings with Initial Two Sections Cooled by Air Flow at Different Speeds (Channel Length=30m)

6 LSM'S NATURAL CONVECTION HEAT TRANSFER BY INCLINED PARALLEL CHANNELS

6.1 Free Convection within Inclined Parallel Channels

Here for computational simplicity, the LSM windings and concrete guideway can be simplified as the horizontal plates. As shown in Figure 10, free air flow can go through the inclined parallel channels between the guideway underneath LSM windings and two guideway trough sides. The "thermal siphon" effect within the passages will result in a natural flow with significant velocity.

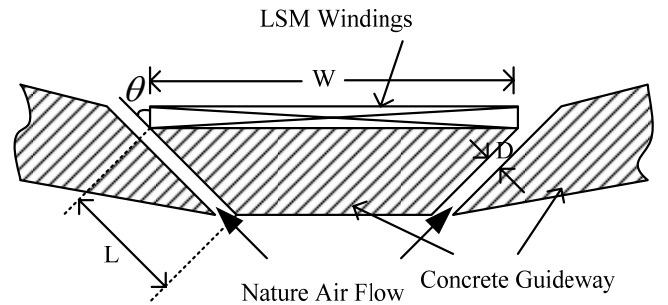


Figure 10. Cross-section View of Inclined Parallel Channels

For asymmetric isoflux conditions with one surface insulated, the maximum Nusselt number may be determined by the following equation [7-8]

$$Nu_s = 0.204[Ra_s(D/L)\cos\theta]^{1/2} \quad (30)$$

where D and L are the width and length of channel, respectively, θ is the inclined degree to the vertical, and Ra_s is the Rayleigh number, which can be given by

$$Ra_s = \frac{g\beta(T_s - T_\infty)D^3}{\nu\alpha} \quad (31)$$

6.2 Combined Free Convection and Radiation Heat Transfer Coefficient

Considering the radiation heat transfer, therefore, the combined free convection of upper heated surface of LSM windings, free convection within the inclined parallel channels, and radiation heat transfer coefficient can be determined by

$$h_c = \frac{k}{L_c} Nu_L + \frac{k}{D} Nu_s + \frac{\varepsilon \sigma [(T_s + 273)^4 - (T_\infty + 273)^4]}{T_s - T_\infty} \quad (32)$$

Figure 11 shows the inclined parallel channel heat transfer coefficient, upper surface heat transfer coefficient, radiation heat transfer coefficient, and combined free convection and radiation heat transfer coefficients vs. temperature difference ΔT from 30°C . It can be seen from the figure that the radiation heat transfer coefficient with the small guideway emissivity of $\varepsilon=0.4$ is about half that of the upper surface, and the inclined parallel channels have almost 4-6 times more efficient heat transfer than the upper surface, so the inclined parallel channels almost dominate the heat transfer. In comparison with the corresponding previous calculation results of heat transfer coefficients, both the radiation heat transfer coefficients and free convection heat transfer coefficient of upper surface are the same, but the inclined parallel channel heat transfer coefficients are about 20 times of the corresponding lower surface heat transfer coefficients of LSM windings.

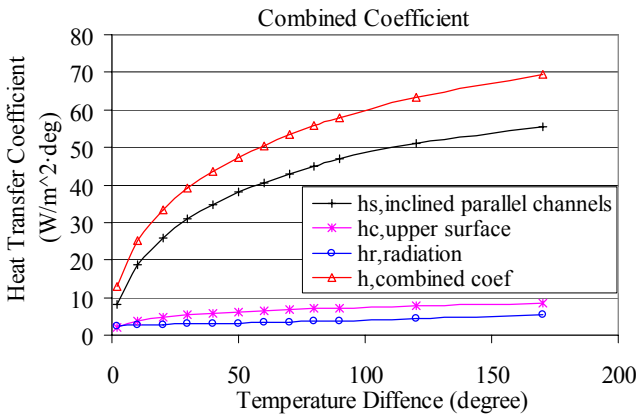


Figure 11: Combined Coefficients vs. Temperature Difference ΔT

6.3 Transient Process

Similarly as the previous simulations of transient process, we assume that an urban 5-section Mag-plane train accelerates to the cruising speed, cruises, and decelerates to a stop for each 3km distance with the headway time of 90s. Figure 12 shows the temperature rise process of the initial four sections of LSM windings and guideway. The temperature is increasing in an exponential way, and it takes almost

14 hours ($\sim 50,000$ seconds) to reach the steady-state temperature.

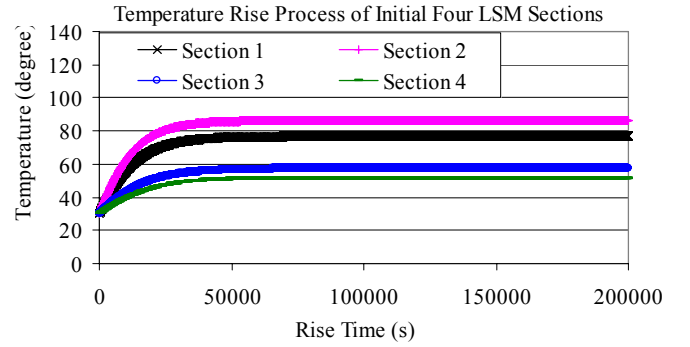


Figure 12: Temperature Rise Process of Initial Four Sections of LSM Windings and guideway

The final steady-state temperature distribution along the initial four sections of LSM windings is shown in Figure 13, and it can be seen from the figure that each section of the LSM windings will be uniformly heated up to the almost same temperature except the two ends which are contiguous to the other section with different temperatures.

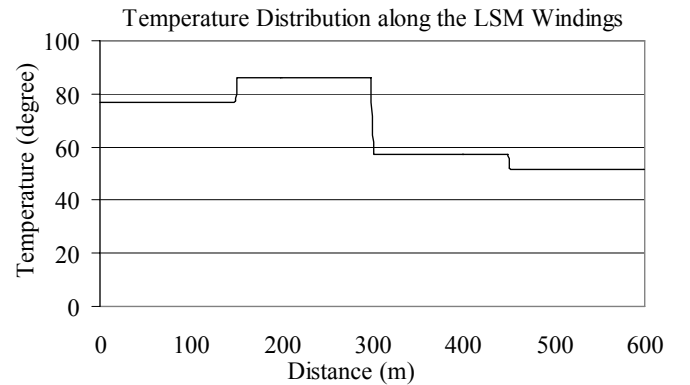


Figure 13: Steady-State Temperature Distribution along the LSM Windings and guideway

It can be seen from Figure 13, that the temperature of both LSM Section 1 and Section 2 are less than the temperature limitation for LSM rubber-insulated cables, and therefore natural convection using inclined parallel channels is a practical solution to solve the temperature rise problem with the initial two sections of the LSM windings and guideway.

7 CONCLUSIONS

The simulation results of LSM's natural convection heat transfer indicated that the temperature rise in the initial two sections of LSM windings and guideway will be more than the allowable temperature limitation for LSM rubber cables if using the short headway of 90s unless some special cooling strategy is adopted. The "thermal siphon" induced natural convection using inclined parallel channels can

solve the temperature rise problem with the initial two sections of LSM windings and guideway.

8 REFERENCES

- Montgomery, D. Bruce, 2004. Overview of the 2004 Magplane Design, *Maglev'2004*, Shanghai, China: 106-113.
- Fang, Jiarong, Radovinsky, Alexey, Montgomery, D. Bruce, 2004. Dynamic Modeling and Control of the Magplane Vehicle, *Maglev'2004*, Shanghai, China: 935-941.
- Magplane International, Inc., 1993. System Concept Definition Report for the National Maglev Initiative, Army Corps of Engineers Contract No. *DTFR53-92-C-00006*, September, 1992; 10 volumes, 1200 pages.
- Cengel, Yunus A. 2003. *Heat Transfer*, Columbus, McGraw Hill.
- Holman, J. P. 1981. *Heat Transfer*, Columbus, McGraw Hill.
- Incropera, Frank P. and DeWitt, David P. 1996. *Fundamentals of Heat and Mass Transfer*, John Wiley & Sons.
- Azevedo, L.F.A. Sparrow, E.M. 1985. Natural Convection in Open-Ended Inclined Channels, *Journal of Heat Transfer*, November Vol. 107, 893-901.
- Incropera, Frank P. and DeWitt, David P. 1996. *Fundamentals of Heat and Mass Transfer*, John Wiley & Sons.